

**ECOC EXHIBITION 2020**



HOME

*ECOC 2020 registration is now open*

Register here for  
ECOC 2020

Get our official conference app

*Whova*

iOS | Android

For Blackberry or Windows Phone [Click here](#)

All times below are Central European Time (at the time of ECOC 2020 this will be UTC+1)

	Sunday 06-Dec	Monday 07-Dec	Tuesday 08-Dec	Wednesday 09-Dec	Thursday 10-Dec
08:00 - 09:00		11 parallel Sessions Mo1A - Mo2B - ... Mo1L	11 parallel Sessions Tu1A - Tu1B - ... Tu1L	11 parallel Sessions We1A - We1B - ... We1L	11 parallel Sessions Th1A - Th1B - ... Th1L
09:30 - 11:00		11 parallel Sessions Mo2A - Mo2B - ... Mo2L	11 parallel Sessions Tu2A - Tu2B - ... Tu2L	11 parallel Sessions We2A - We2B - ... We2L	11 parallel Sessions Th2A - Th2B - ... Th2L
13:30 - 15:00	Workshops WS1 - WS2 - ... - WS 14	13:45 - 14:00	Opening Session	Tutorials (1-6)	Tutorials (1-6) (repeated)
		14:00 - 14:15			
14:15 - 15:15					
15:30 - 17:00	Workshops WS1 - WS2 - ... - WS 14	Plenary Presentations 3 & 4	Tutorial (7-11) & Demo Session	Tutorial (7-11) & Demo Session (repeated)	Closing Session
18:00 - 19:00		11 parallel Sessions Mo1A - Mo2B - ... Mo1L	11 parallel Sessions Tu1A - Tu1B - ... Tu1L	11 parallel Sessions We1A - We1B - ... We1L	11 parallel Sessions Th1A - Th1B - ... Th1L
19:30 - 21:00		11 parallel Sessions Mo2A - Mo2B - ... Mo2L	11 parallel Sessions Tu2A - Tu2B - ... Tu2L	11 parallel Sessions We2A - We2B - ... We2L	11 parallel Sessions Th2A - Th2B - ... Th2L



	Room A	Room B	Room C	Room D	Room E	Room F	Room G	Room H	Room J	Room K	Room L
08:00 -- 09:00	We1A - Scattering, coupling and sensing	We1B - Lasers	We1C - Transmitters and receivers	We1D - Machine learning for transceivers	We1E - Novel concepts in optical communications	We1F - Shaping-based communications	We1G - Satellite communications	We1H - Network performance monitoring	We1J - Optical Access Networks and 5G I	We1K - Network Control and Management	We1L - Neuromorphic Computing
<b>Break</b>											
09:30 -- 11:00	We2A - Nonlinear Optics	We2B - Detectors	We2C - Complex integrated optic circuits	We2D - Equalizers and decoders for IMDD systems	We2E - Unrepeated transmission	We2F - Long haul transmission	We2G - Free Space Optics	We2H - High-capacity network architecture	We2J - Optical Access Networks and 5G II	We2K - Network Planning	We2L - Nano and quantum photonics
11:00 -- 12:00	<b>BreakBreak</b>										
12:00 -- 12:30	<b>DEMO Session (repeated)</b>	<b>11th European Photonic Integration Forum at ECOC 2020 - The bigger PIC news with Kevin and Roel</b>	<b>Future developments and trends in optical networks – a perspective by the editors of the Springer Handbook of Optical Networks</b>								
12:30 -- 13:00		<b>Break</b>									
14:00 -- 15:00	Tutorial SC01	Tutorial SC02	Tutorial SC03	Tutorial SC04	Tutorial SC05	Tutorial SC06					
<b>Break</b>											
15:30 -- 16:30							Tutorial SC07	Tutorial SC08 (withdrawn)	Tutorial SC09	Tutorial SC10	Tutorial CLEO
16:30 -- 17:30	<b>Educational Worldwide Lab Tour (Room A)</b>										

## Session We2C: Complex integrated optic circuits

Wednesday 09 December 2020 09:30 - 11:00 (AM Session) & 19:30 - 21:00 (PM Session)

Chair AM-session: Bottoni, Fabio

Chair PM-session: Augustin, Luc

09:30 (AM Session) & 19:30 (PM Session)

### **We2C-1: (Extended) 2x800Gbps/wave Coherent Optical Module Using a Monolithic InP Transceiver PIC**

Chitgarha, Mohammad Reza; Studenkov, Pavel; Zhang, Jiaming; Hodaei, Hossein; Frost, Thomas; Tsai, Huan-Shang; Buggaveeti, Sanketh; Rashidinejad, Amir; Yekani, Amin; Mirzaei Nejad, Reza; Kerns, Samantha; Diniz, Júlio; Pavinski, Don; Brigham, Robert; Foo, Ben; Al-Khateeb, Mohammad; Koenig, Swen; Wolf, Stefan; Going, Ryan; Porto, Stefano; Leung, Irene; Maher, Robert; Dominic, Vince; Sun, Han; Sanders, Steve; Osenbach, John; Corzine, Scott; Evans, Peter; Lal, Vikrant; Ziari, Mehrdad Ziari  
*Infinera Corp. (USA)*

**Abstract:** We report on the development of a 2x800Gbps/wave coherent module based on a monolithic InP transceiver PIC and real-time 7nm DSP ASIC capable of 800Gbps data transmission over record 1000km SMF-28 link using a 96Gbaud, PCS-64QAM modulation format.

10:00 (AM Session) & 20:00 (PM Session)

### **We2C-4: A Compact Monitoring Circuit to Accurately Extract Fabrication Deviation in Silicon Waveguides**

Horikawa, Tsuyoshi; Okayama, Hideaki; Onawa, Yosuke; Shimura, Daisuke; Ushida, Jun; Shiina, Akemi; Murao, Tadashi; Yaegashi, Hiroki  
*Photonics Electronics Technology Research Association (PETRA) (Japan)*

**Abstract:** Novel optical circuit with a microring resonator and polarization rotators was proposed for process control monitoring. The extraction method by TE and TM spectral analysis using the circuit showed sensitivity to sub-nm order fabrication deviations as well as robustness to measurement errors.

10:10 (AM Session) & 20:10 (PM Session)

### **We2C-5: An Accurate and Computationally Efficient Large-signal SPICE Model for Depletion-type Silicon Ring Modulators Including Temperature Dependence**

Kim, Minkyu (1); Lischke, Stefan (2); Mai, Christian (3); Zimmermann, Lars (4); Choi, Woo-Young (1)

(1) Yonsei University (South Korea), (2) IHP GmbH (Germany), (3) IHP (Germany), (4) Technische Universität Berlin (Germany)

**Abstract:** We present large-signal SPICE model for ring modulators including temperature dependence. The model is verified with 25-Gb/s NRZ modulation at several different temperatures. With this model, the temperature-dependent eye diagrams together with the temperature control IC is successfully simulated in the standard IC design environment.

10:20 (AM Session) & 20:20 (PM Session)

### **We2C-6: Polarization-insensitive low-crosstalk 8 × 8 silicon photonics switch with 9 × 13.5 cm<sup>2</sup> control board**

Konoike, Ryotaro; Matsuura, Hiroyuki; Suzuki, Keiji; Kawashima, Hitoshi; Ikeda, Kazuhiro  
*National Institute of Advanced Industrial Science and Technology (AIST) (Japan)*

**Abstract:** An on-chip polarization-diversity 8 × 8 silicon photonics switch with PDL < 0.4 dB, DGD < 1.8 ps and crosstalk < -30 dB over 70-nm bandwidth is demonstrated. The USB-controlled switch module has a compact size of 9 × 13.5 cm<sup>2</sup>.

# An Accurate and Computationally Efficient Large-signal SPICE Model for Depletion-type Silicon Ring Modulators Including Temperature Dependence

Minkyu Kim<sup>(1)</sup>, Stefan Lischke<sup>(2)</sup>, Christian Mai<sup>(2)</sup>, Lars Zimmermann<sup>(2),(3)</sup>, and Woo-Young Choi<sup>(1)</sup>

<sup>(1)</sup> Yonsei University, 03722 Seoul, South Korea, [minkyu226@yonsei.ac.kr](mailto:minkyu226@yonsei.ac.kr)

<sup>(2)</sup> IHP, Im Technologiepark 25, 15236 Frankfurt (Oder), Germany

<sup>(3)</sup> Technische Universitaet Berlin, Einsteinufer 25, 10587 Berlin, Germany

**Abstract** We present large-signal SPICE model for ring modulators including temperature dependence. The model is verified with 25-Gb/s NRZ modulation at several different temperatures. With this model, the temperature-dependent eye diagrams together with the temperature control IC is successfully simulated in the standard IC design environment.

## Introduction

Depletion-type Si ring modulators (RMs) attract a great amount of research and development interests because they can provide superior performances for demanding optical interconnect applications with their large modulation bandwidth, small-footprint, and energy-efficient operation<sup>[1]</sup>. However, their performance is highly dependent on the temperature, so the RM temperature control (TC) that provides the stable and optimal modulation characteristics is an absolute necessity for any practical application of Si RMs<sup>[2]–[4]</sup>. Furthermore, the performance of the entire transmitter is greatly influenced by the modulator driving electronics. Consequently, for any optical interconnect application of Si RMs, there is a great demand for the capability of temperature-dependent electro-photon co-simulation of RMs together with drivers and temperature controllers during the initial design stage preferably in the standard IC design environment<sup>[5], [6]</sup>. Previously, we demonstrated a large-signal SPICE model for Si RM that is easy-to-use in the standard IC design platform and allows accurate co-simulation of the RM and the driver circuit<sup>[7]</sup>. We expand this model by adding temperature dependence and demonstrate accurate SPICE-level simulation of the Si transient modulation characteristics together with the TC circuit.

## Temperature-dependent Si RM parameters

The key parameters for describing the Si RM optical behavior are the effective index of the waveguide ( $n_{eff}$ ), the field ratio after one round-trip in the ring waveguide ( $\alpha$ ), and the coupling coefficient in the directional coupler between the ring and bus waveguide ( $\gamma$ ). The RM transmission characteristics is determined by these three parameters in the following manner,

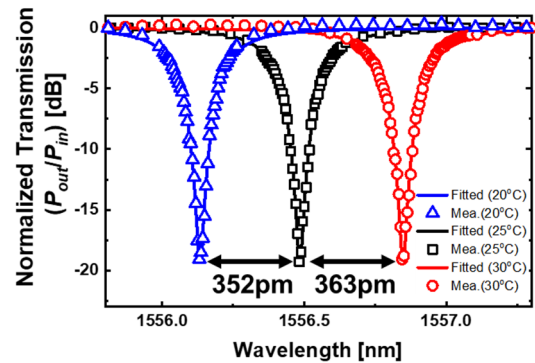


Fig. 1: Measured and fitted transmission curve for different operating temperatures at Voltage=0 V

$$T = \frac{P_{out}}{P_{in}} = \frac{\alpha^2 - 2\alpha\gamma\cos(\phi) + \gamma^2}{1 - 2\alpha\gamma\cos(\phi) + (\alpha\gamma)^2}, \quad (1)$$

where  $\phi = \frac{2\pi n_{eff}}{\lambda} L_{ring}$  and  $L_{ring}$  is the ring

circumstance. In order to determine temperature dependence of these three parameters, transmission characteristics of a sample Si RM are measured at three different temperatures and the results are shown in Fig. 1. The measured Si RM is fabricated in IHP's Si PIC technology. It has 8 $\mu$ m radius and 290nm gap between ring and bus waveguides. As shown in the figure, the resonance wavelength linearly shifts with temperature. The measured temperature dependence of 70 pm/ $^{\circ}$ C agrees well with the value calculated from the Si thermo-optic coefficient. The temperature dependence of  $n_{eff}$  can be determined from the resonance condition,  $m\lambda_{res} = n_{eff} L_{ring}$ , and the resulting  $n_{eff}$  values are

Table 1: Extracted parameters of Si RM with different temperatures at Voltage=0 V

Temperature	$n_{eff}$	alpha	gamma
20 $^{\circ}$ C	2.631470	0.9804	0.985
25 $^{\circ}$ C	2.632066		
30 $^{\circ}$ C	2.632679		

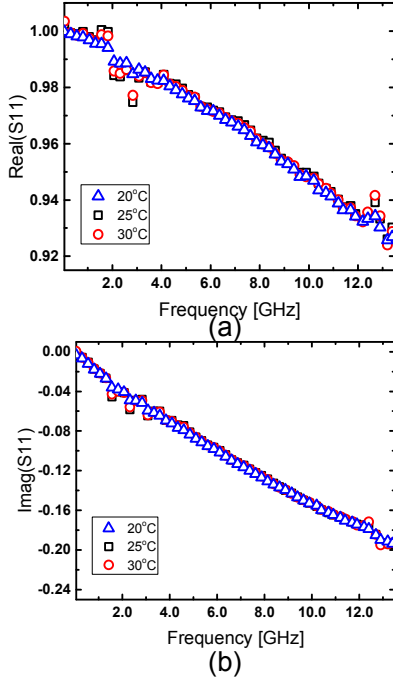


**Fig. 2:** Measured reflection coefficient (S11) of the Si RM, (a) real part and (b) imaginary part for different temperatures at Voltage=0 V

shown in Table 1. Numerical values for  $\alpha$  and  $\gamma$  for different temperatures can be determined by fitting Eq. (1) to the measured transmission characteristics but there is very little change for  $\alpha$  and  $\gamma$  within the temperature range investigated here. Their numerical values are given in Table 1. With these results,  $n_{eff}$  can be regarded as the only temperature-dependent optical parameter for RM transmission characteristics.

Electrical characteristics of the Si RM such as series resistance ( $R_s$ ) and p-n junction capacitance ( $C_j$ ) also influence the Si RM modulation frequency response. Fig. 2 shows the measured reflection coefficient (S11) of the sample Si RM at different temperatures. As can be seen in the figure, there is very little change with temperature. Consequently, we can assume the Si RM electrical parameters do not change with temperature within the temperature range of interest.

### Large-signal SPICE model with temperature dependence

The previously reported large-signal SPICE model<sup>[7]</sup> of the Si RM is based on the small-signal frequency modulation response derived from the RM coupled-mode equations given as

$$\frac{s + (2/\tau_l)}{s^2 + (2/\tau)s + D^2 + (1/\tau^2)}, \quad (2)$$

where  $D$  is the difference between the input light

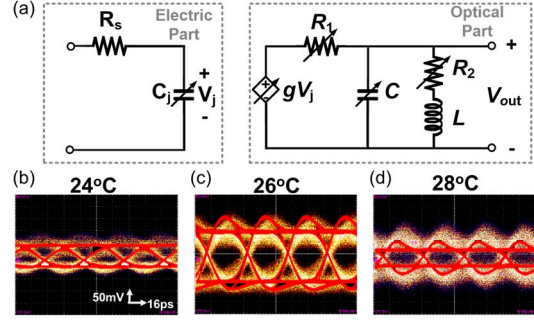


**Fig. 3:** (a) SPICE model and (b-d) its verification with NRZ 25-Gb/s data at different temperatures

wavelength and the resonance wavelength,  $\tau_l$  and  $\tau$  are the time-constants due to the ring waveguide loss and the total loss including coupler loss, respectively.  $\tau_l$  and  $\tau$  are related to  $\alpha$  and  $\gamma$  as

$$\frac{1}{\tau_l} = \frac{(1-\alpha^2)c}{2n_{eff}L_{ring}}, \quad \frac{1}{\tau} = \frac{(2-\alpha^2-\gamma^2)c}{2n_{eff}L_{ring}}. \quad (3)$$

Eq. (2) can be represented with an RLC circuit shown in the right side of Fig. 3(a). The R,L,C values can be obtained by matching Eq. (2) to the transfer function of the RLC circuit. Together with the left side block representing the electrical frequency response, the circuit in Fig. 3(a) is the equivalent circuit for the RM modulation characteristics. In the equivalent circuit, variable electrical components are used since their values depend on the voltage applied to the Si RM. In short, by extracting numerical values for voltage-dependent  $\alpha$ ,  $\gamma$ ,  $n_{eff}$  at different temperatures and with the given values of  $D$  and  $L_{ring}$ , all the circuit element values in Fig. 3(a) can be determined and, using the equivalent circuit, the entire large-signal Si RM modulation characteristics can be efficiently simulated in SPICE. Fig. 3(b),(c),(d) show such simulated results at three different temperatures along with measured results. For the simulation, voltage-dependent parameters are modeled with the third-order polynomials and temperature dependence of  $n_{eff}$  is linearly modeled. With 25-Gb/s  $2^{31}-1$  PRBS NRZ input data having  $4-V_{peak-to-peak}$  swing, the resulting equation-based R,L,C values allow very efficient SPICE simulation at a given temperature, the result of which agrees well with the measurement result.

### RM Co-simulation with TC IC

The real advantage of our model is the ease with which it can be used for co-simulation of RMs and electronic circuits such as TC IC. The lower block in Fig. 4 shows the block diagram of the RM TC IC fabricated in IHP's BiCMOS platform<sup>[3]</sup>. Fig. 5 shows the co-simulation results for the RM with this TC IC. For the simulation, the RM is

## Conclusion

We present a large-signal SPICE model for the Si RM including temperature dependence. With our model, electro-optic co-simulation of the Si RM with and electronic circuit is possible. In particular, we demonstrate that temperature-dependent Si RM eye-diagrams can be simulated together with the TC IC. Our model should be of great use for any Si electro-photonic integrated circuits including RMs.

## Acknowledgements

This work is supported by the Ministry of Trade, Industry and Energy (MOTIE) (10065666); National Research Foundation of Korea (NRF) grant funded by Korea Government (MSIT) (2020R1A2C201508911). Also, we thank IC Design Education Center (IDEC) for EDA tool support.

## References

- [1]H. Li *et al.*, "A 112 Gb/s PAM4 Transmitter with Silicon Photonics Microring Modulator and CMOS Driver," in *Optical Fiber Communication Conference Postdeadline Papers* 2019, 2019, vol. 2, p. Th4A.4.
- [2]C. Sun *et al.*, "A 45 nm CMOS-SOI Monolithic Photonics Platform With Bit-Statistics-Based Resonant Microring Thermal Tuning," *IEEE J. Solid-State Circuits*, vol. 51, no. 4, pp. 893–907, Apr. 2016.
- [3]M.-H. Kim, L. Zimmermann, and W.-Y. Choi, "A Temperature Controller IC for Maximizing Si Micro-Ring Modulator Optical Modulation Amplitude," *J. Light. Technol.*, vol. 37, no. 4, pp. 1200–1206, Feb. 2019.
- [4]M. Kim *et al.*, "A Fully Integrated 25 Gb/s Si Ring Modulator Transmitter with a Temperature Controller," in *Optical Fiber Communication Conference (OFC) 2020*, 2020, p. T3H.7.
- [5]B. Wang *et al.*, "A Compact Verilog-A Model of Silicon Carrier-Injection Ring Modulators for Optical Interconnect Transceiver Circuit Design," *J. Light. Technol.*, vol. 34, no. 12, pp. 2996–3005, 2016.
- [6]J. Rhim, Y. Ban, B.-M. Yu, J.-M. Lee, and W.-Y. Choi, "Verilog-A behavioral model for resonance-modulated silicon micro-ring modulator," *Opt. Express*, vol. 23, no. 7, pp. 8762–8772, 2015.
- [7]M. Kim *et al.*, "Large-signal SPICE model for depletion-type silicon ring modulators," *Photonics Res.*, vol. 7, no. 9, p. 948, Sep. 2019.

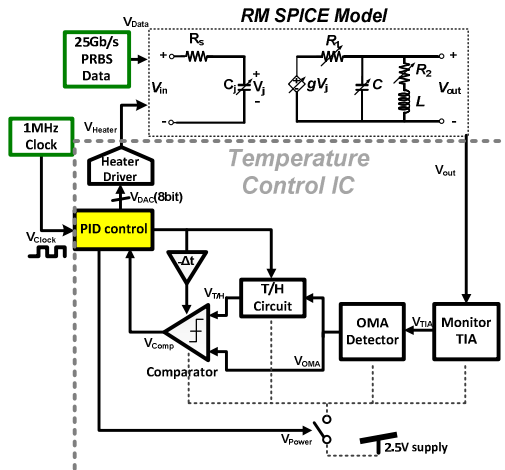


Fig. 4: Block diagram for co-simulation with SPICE model and temperature control IC

continuously modulated with 25-Gb/s  $2^{31}-1$  PRBS data and the RM output power is obtained with 1-ps resolution, which is shown in Fig. 5(a) with magenta lines and 10ns zoomed-in data is shown as well. Initially, the TC IC provides a temperature scan of the RM with the on-chip heater with 1-MHz clock update, and the RM OMA is monitored, where the OMA value is labeled with red lines. The TC IC determines the largest OMA (marked B in Fig. 5(a)) and controls the RM temperature so that this OMA is maintained. Simulated eye diagrams are also shown for three different points in Fig. 5(b), which shows that Point B has the largest OMA compared to the other points. With the RM SPICE model, such temperature-aware simulation was possible within three hours for over  $100\mu\text{s}$  simulation with 1ps resolution, which is much computationally efficient compared to Verilog-A model. With such simulation, we can provide feasibility of the co-simulation with temperature control IC as well as the RM's dynamics along the time-variant temperature, and this can extend to co-simulation with other complicated environments such as thermal perturbation due to the chip power dissipation.

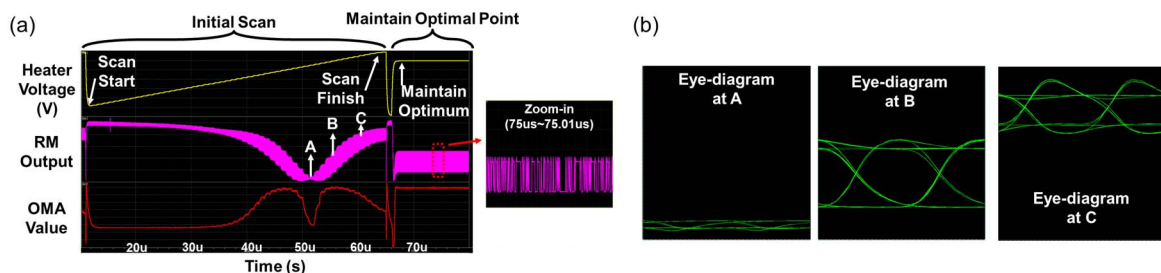


Fig. 5: Co-simulation with SPICE model and temperature control IC